Research Article

Structure-Based Virtual Screening of Bitter Almond Phytochemicals Against PARP1

Sneha Yadav[1], Brijesh sirohi [2] , Naveen Gupta[3] , Pinky Singh[4], Neeraj Kumar Shrivastava[5] , Dr. Suraj Kumar Prajapati[6]

[1]Madhyanchal Professional University, Madhya Pradesh, ORCID ID - 0000-0002-4378-922X
[2]Radharaman college of pharmacy, Bhopal, Madhya Pradesh, ORCID ID - 0009-0006-7913-1530
[3]Madhyanchal Professional University, Madhya Pradesh
[4]Madhyanchal Professional University, Madhya Pradesh, ORCID ID - 0009-0001-4627-8564
[5]Amity Institute of Pharmacy, Gwalior, Madhya Pradesh, ORCID ID - 0009-0006-0229-3937
[6]Ambedkar Institute of higher education. Pharmacy Division. Patna, Bihar India. ORCID ID - https://orcid.org/0000-0002-2612-6176

Abstract

Background: Poly(ADP-ribose) polymerase-1 (PARP1) is a key DNA repair enzyme involved in maintaining genomic integrity and regulating cellular responses to oxidative stress. Aberrant PARP1 activation has been implicated in the pathogenesis of cancer and several chronic diseases, making it an attractive therapeutic target. Natural phytochemicals from Prunus dulcis var. amara (bitter almond) possess diverse biological activities; however, their inhibitory potential against PARP1 has not been comprehensively investigated.

Methods: Phytochemicals reported from Prunus dulcis var. amara were identified through an extensive literature survey and verified using the PubChem database. The selected compounds were prepared using the LigPrep module of Schrödinger Suite and docked against the catalytic domain of human PARP1 (PDB ID: 2RCW) using Glide. Binding stability was further evaluated through Prime MM/GBSA binding free energy calculations. Protein–ligand interactions were analyzed using two-dimensional interaction diagrams. Based on the computational findings, quercetin was further evaluated for in vitro PARP1 inhibitory activity.

Results: Molecular docking demonstrated that all investigated phytochemicals exhibited favorable binding within the catalytic pocket of PARP1. Epigallocatechin gallate showed the highest docking affinity (Glide score: −11.5 kcal/mol), followed by isoquercetin (−10.5 kcal/mol), quercetin (−9.1 kcal/mol), and vicenin-2 (−8.8 kcal/mol). MM/GBSA analysis identified isoquercetin as the most stable ligand–protein complex with a binding free energy of −67.52 kcal/mol, followed by quercetin (−49.76 kcal/mol), prunasin (−45.46 kcal/mol), and vicenin-2 (−42.87 kcal/mol). Protein–ligand interaction analysis revealed extensive hydrogen-bonding and hydrophobic interactions with key residues within the PARP1 catalytic site, supporting the observed binding affinities. Furthermore, quercetin demonstrated significant in vitro PARP1 inhibitory activity with an IC_{50} value of 2.32 ± 0.18 µM, corroborating the computational predictions.

Conclusion: The present study demonstrates that phytochemicals from Prunus dulcis var. amara, particularly isoquercetin, quercetin, vicenin-2, and epigallocatechin gallate, exhibit promising inhibitory potential against PARP1. The integration of molecular docking, MM/GBSA binding energy analysis, protein–ligand interaction profiling, and in vitro validation highlights these natural compounds as potential lead molecules for the development of novel PARP1-targeted therapeutics. Further molecular dynamics simulations and preclinical investigations are warranted to confirm their therapeutic potential.

Keywords: Prunus dulcis var. amara; Bitter almond; PARP1; Molecular docking; MM/GBSA; Phytochemicals; Quercetin; Isoquercetin; Polyphenols; DNA repair.

Introduction

Poly ADP-ribose polymerase 1(PARP1), also known as ADPRT1 plays a significant role in DNA repair, which serves as a catalyst for the polymerization of ADP-ribose units derived from NAD^+ results in attachment of ADP-ribose to proteins (1). Arginine, glutamate, aspartate, cysteine, lysine, and serine are among the amino acids to which PARP1 attracts ADP-ribose moieties (2). Attachment of these amino acids to ADP-ribose moieties is essential for repair of DNA-damage hence helps in remodelling of chromatin (3).

By coordinating several DNA repair pathways, including the base excision repair (BER) and single-strand break repair (SSBR) pathways, PARP1, a crucial DNA damage sensor and repair enzyme, plays a crucial role in preserving genomic integrity. When oxidative stress, ionizing radiation, or alkylating chemicals cause DNA single-strand breaks, PARP1's zinc-finger DNA-binding domains quickly identify and attach to the damaged DNA. By employing nicotinamide

(NAD^+) as a substrate, this contact triggers its catalytic function, which results in the production of poly(ADP-ribose) (PAR) chains (4, 5). In order to efficiently repair damaged DNA, the PAR chains function as molecular signals that attract and assemble necessary DNA repair proteins, such as X-ray repair cross-complementing protein 1 (XRCC1), apurinic/apyrimidinic endonuclease 1 (APE1), DNA polymerase β, DNA ligase III, and polynucleotide kinase phosphatase (PNKP). In addition to its main function in BER and SSBR, PARP1 modulates chromatin structure and encourages the recruitment of DNA repair complexes at double-strand break sites, which helps regulate homologous recombination (HR), non-homologous end joining (NHEJ), and alternative non-homologous end joining (Alt-NHEJ). PARP1-dependent cell death (parthanatos), cellular energy depletion, and mitochondrial malfunction are caused by sustained PARP1 activation under conditions of severe oxidative stress, which leads to the overconsumption of NAD^+ and ATP. As a result, PARP1 is a viable therapeutic target for illnesses like cancer, neurological disorders, cardiovascular diseases, and chronic inflammatory conditions that are marked by oxidative DNA damage (6).

The tryptophan-glycinearginine-rich domain, a CAT domain, an auto modification domain, and an N-terminal DNA binding domain make up PARP1 (7). The HD and ART subdomains make up the CAT domain. PARP1 activity may be inhibited by the identification of a small chemical that can target the catalytic location on the interaction surface of these two subdomains. Olaparib (8), Rucaparib (9), Niraparib (10), and Talazoparib (11,12) are the four FDA-approved PARP1 inhibitors at this time. There are also a number of inhibitors undergoing preclinical and clinical research (13-20). Benzamide structures are present in the majority of PARP1 inhibitors, which imitate nicotinamide's competitive binding of PARP1 to NAD+ at the nicotinamide-ribose binding domain (NI site) of the PARP1 catalytic domain.

The structural variety of natural chemicals makes them an important source of new drugs. Natural chemicals are the source of more than 32% of small molecule medications sold between 1981 and 2019 (21). Natural substances with a variety of pharmacological properties are abundant in traditional Chinese remedies. Among these, Huangbai, Baixianpi, and Shechuangzi have been utilized for over a millennium and are well-known for their antibacterial, anti-inflammatory, and anti-tumor properties. One quick method is to combine bioactivity testing and molecular modeling to identify specific inhibitors from natural substances (22, 23, 24).

In this study, we extracted the chemical components of Prunus dulcis var amara and used molecular docking to identify possible PARP1 inhibitors. PARP1 enzyme testing revealed four PARP1 potential inhibitors. Ultimately, the interactions between PARP1 and the potential chemical inhibitors were clarified from both structural and energetic viewpoints using molecular dynamics simulation and free energy computation. These potential substances show promise for the creation of treatments that target disorders linked to PARP1.

2.0 Material and Methods

2.1 Collection of Phytochemical Constituents of PDVA

The phytochemical constituents of PDVA were compiled through a comprehensive literature survey and data mining of publicly available phytochemical databases. Information on the phytochemical composition was collected from peer-reviewed research articles, review papers, and other scientific publications describing the phytochemical profile, nutritional composition, antioxidant properties, and pharmacological activities of bitter almond. The collected phytochemicals were further cross-verified using the PubChem database to confirm their molecular structures, chemical names, Simplified Molecular Input Line Entry System (SMILES) notations, and PubChem Compound Identifiers (CID).

The identified phytochemicals comprised diverse classes of secondary metabolites, including flavonoids, phenolic acids, cyanogenic glycosides, phytosterols, fatty acids, terpenoids, and other polyphenolic constituents reported in Prunus dulcis var. amara. Based on their documented antioxidant, anti-inflammatory, anticancer, and cytoprotective properties, representative phytochemicals were selected for molecular docking studies against the catalytic domain of PARP1. 2D structures of the selected compounds were retrieved from the PubChem database in Structure Data File (SDF) format and subsequently used for ligand preparation prior to molecular docking analysis (25,26, 27, 28).

2.2 Structural based Screening

2.2.1 Protein Preparation

The structural coordinates, established through X-Ray crystallography, of the targets were located and extracted from the RCSB Protein Data Bank (2RCW), and subsequently imported into Schrodinger Maestro. Within the Schrodinger software, the proteins underwent preparation via a three-step procedure facilitated by the protein preparation wizard. During preprocessing, the imported structure underwent refinement, including the removal of heteroatoms and crystallographic waters, and optimization of hydrogen bonds to achieve a low-energy state at a pH of 7.4 using the OPLS3e force field. The structures of the previously acquired bioactives, intended for predicting biological targets, were optimized for three-dimensional coordinates using the LigPerp application integrated into Schrodinger. The potential ionization states of the ligands were generated using the Epik tool, and tautomeric states were produced for each ligand before saving the results (29).

2.2.2 Molecular Docking and MMGBSA

The receptor grid was generated surrounding the co-crystallized ligand. In cases where proteins didn't have a co-crystallized ligand, site map was used to identify and assess the binding pocket. For such targets (proteins), the receptor grid generation was done with an entry option to form a grid on the site with the maximum SiteScore, containing crucial amino acid residues essential for regulating protein activity. Rigid XP-docking was conducted to assess and prioritize potential components, and the outcomes were visualized using an XP-visualizer. Prime MM-GBSA analysis was conducted determine the binding free energy. Subsequently, protein and ligand complexes with favorable docking scores, binding free energy, and significant interactions as indicated by XP-dock results were selected for MD simulation (30).

2.3 In-vitro PARP1 enzymatic Assay

All chemicals and reagents were of analytical grade and procured from Sigma-Aldrich (Merck Life Science Pvt. Ltd., Bengaluru, Karnataka, India), HiMedia Laboratories Pvt. Ltd. (Mumbai, Maharashtra, India), and SRL Pvt. Ltd. (Mumbai, Maharashtra, India). The inhibitory activity all targeted compounds were determined against PARP1 enzyme by spectrophotometric method by ELISA in 96-well plates. These wells are precoated with histones which is diluted in 100µL PBS buffer and incubated overnight at 4 °C. Thereafter we put 100µM NAD^+ which is diluted in 30µl Tris buffer solution adjusted at pH 8, further 25 µM biotinylated NAD+ , and 200 nM sDNA were added to each well, and then 5µL of compound or solvent control was added at varying concentrations. Then 20µL PARP1 enzyme was added at 30°C and 50µL of HRP was added after 1h. After 30min, the luminescent signal was measured using a multiwall spectrophotometer (Molecular device SpectraMax M5 microplate reader) (31).

3.0 Results & Discussion

3.1 Identification of Phytochemical Constituents of PDVA

Fourty two phytochemical compounds reported in PDVA were found after a thorough review of the literature and a search of phytochemical databases. Flavonoids, phenolic acids, cyanogenic glycosides, phytosterols, fatty acids, terpenoids, and other polyphenolic ingredients were among the several types of secondary metabolites represented by the discovered substances (Supplementary Table S1).

Based on their documented antioxidant, anti-inflammatory, anticancer, and cytoprotective properties reported in the literature, quercetin, kaempferol, isoquercetin, vicenin-2, naringin, amygdalin, prunasin, catechin, chlorogenic acid, gallic acid, β-sitosterol, stigmasterol, oleic acid, palmitic acid, and mangiferin were chosen for additional molecular docking studies. Before ligand production, the chemical structures of all the chosen compounds were successfully obtained from the PubChem database and confirmed using their matching PubChem Compound Identifiers (CID).

The chosen phytochemicals, which included polyphenols, flavonoid glycosides, cyanogenic glycosides, phytosterols, and fatty acids, demonstrated significant structural diversity, offering a chemically varied ligand library for virtual screening against PARP1. This variety made it possible to assess various molecular scaffolds that might interact with PARP1's catalytic binding region. Molecular docking was then applied to the constructed ligand library in order to determine which compounds had the highest binding affinity toward the PARP1 active site.

3.2 Molecular Docking Analysis

3.2 Molecular Docking Analysis

The binding affinity of the chosen phytochemicals from PDVA to the catalytic domain of PARP1 (PDB ID: 2RCW) was assessed using molecular docking. With docking scores ranging from −7.1 to −11.5 kcal/mol, all of the chosen phytochemicals were successfully accommodated within the active-site cavity of PARP1, according to the docking study (Table 2,).

With a Glide docking score of −11.5 kcal/mol, epigallocatechin gallate (EGCG) showed the highest docking affinity among the screened compounds, followed by vicenin-2 (−8.8 kcal/mol), isoquercetin (−10.5 kcal/mol), and quercetin (−9.1 kcal/mol). The remaining phytochemicals showed significant binding to the catalytic pocket of PARP1, including amygdalin (−7.9 kcal/mol), β-sitosterol (−7.5 kcal/mol), prunasin (−7.3 kcal/mol), kaempferol (−7.2 kcal/mol), and rutin (−7.1 kcal/mol).

Prime MMGBSA binding free energy calculations were carried out to assess the docked complexes' stability in further detail. According to the findings, isoquercetin had the best binding free energy (ΔGbind = −67.52 kcal/mol), suggesting the creation of a very stable ligand–protein complex. Strong binding free energies were also shown by quercetin (−49.76 kcal/mol), prunasin (−45.46 kcal/mol), vicenin-2 (−42.87 kcal/mol), β-sitosterol (−41.68 kcal/mol), and amygdalin (−41.30 kcal/mol). Despite having excellent docking scores, kaempferol (−35.61 kcal/mol), rutin (−35.58 kcal/mol), and epigallocatechin gallate (−32.38 kcal/mol) showed much less favorable MM/GBSA binding energies.

The most promising phytochemicals against PARP1 were found to be isoquercetin, quercetin, vicenin-2, and epigallocatechin gallate, according to the molecular docking and MM/GBSA studies. Isoquercetin showed the best binding free energy, indicating the creation of a more stable ligand–protein complex, even though epigallocatechin gallate had the highest docking score. These results suggest that bitter almond flavonoid-based phytochemicals have strong PARP1 binding potential and could be useful lead compounds for additional molecular dynamics simulations and experimental verification.

Table 2: Representing the docking score and MMGBSA (ΔG) Bind scores

Protein	PDB ID	Compound	Docking Score	MMGBSA (ΔG)
PARP1	2RCW	Quercetin	-9.1	-49.76
		Vicenin-2	-8.8	-42.87
		Amygdalin	-7.9	-41.3
		isoquercetin	-10.5	-67.52
		kaempferol	-7.2	35.61
		Epigallocatechin gallate	-11.5	-32.38
		Rutin	-7.1	-35.58
		prunasin	-7.3	-45.46
		β-sitosterol	-7.5	-41.68

3.3 Protein–Ligand Interaction Analysis

To comprehend the molecular underpinnings of ligand recognition and complex stabilization, the binding interactions between the chosen phytochemicals and the catalytic pocket of PARP1 were further examined. Table 3 summarizes the docked complexes' interaction profiles, which include hydrogen bonds, hydrophobic interactions, π–π stacking, π-cation interactions, water bridges, and van der Waals contacts.

In line with its highest MMGBSA binding free energy (−67.52 kcal/mol), isoquercetin demonstrated the greatest number of advantageous interactions with residues situated within the PARP1 binding pocket, forming numerous hydrogen bonds along with extensive hydrophobic contacts. Additionally, quercetin and vicenin-2 formed a number of hydrogen-bonding contacts with residues in the active site, which helped them achieve stable binding conformations and favorable docking scores.

Despite having the best docking score (−11.5 kcal/mol), epigallocatechin gallate produced relatively few stabilizing contacts, which could account for its lower MM/GBSA binding free energy. Similarly, amygdalin and prunasin formed

hydrogen bonds through their hydroxyl-rich glycosidic moieties, while β-sitosterol mostly interacted through hydrophobic contacts due to its steroidal structure. According to the interaction patterns, hydrophobic and hydrogen bonding interactions are crucial for maintaining ligand binding in PARP1's catalytic domain. Overall, the interaction analysis showed that compared to the other phytochemicals, flavonoid derivatives generated stronger and more extensive interaction networks, which supported their higher binding affinity toward PARP1.

Table 3: Representing the bonding and non-bonding interactions of compounds of the targets

Protein	Compound	Bonding and Non-Bonding Interactions
2RCW	Quercetin	**H-Bond**-ARG-25, ARG-23, TYR-18, ILE-19 **Salt-Bridge**-ARG-23 Charged positive-ARG-86, LYS-39, LYS-14 **Charged negative**-GLU-17 **Polar**- ASN-53, ASN-54 **Hydrophobic**- LEU-52, PRO-24
	Vicenin-2	**H-Bond**- ARG-86, GLU-17, ILE-19 **Charged positive-** ARG-23, ARG-25 Polar- ASN-53 **Hydrophobic**- LEU-52, ILE-84 **Glycine**-GLY-16
	Amygdalin	**H-Bond** - ASN-53, LEU-52, ARG-86, ARG-23, LYS-14 **Salt-Bridge**-ARG-25, LYS-14 **Charged positive**-ARG-15 **Charged negative**-GLU-17 **Polar**-GLN-79, ASN-54 **Hydrophobic**-PHE-55, ILE-84, ILE-19, 1YR-18 **Glycine**-GLY-16
	isoquercetin	**H-Bond-** ASP-200, ASP-133, ARG-141, GLN-185, ASN-186 **Charged positive**- LYS-85, LYS- 183 **Polar-** THR-138 **Hydrophobic-** LEU-188, LEU-132, CYS-199, ILE-62, VAL-70, VAL-110, VAL-135, ALA-83, TYR-134
	kaempferol	**H-Bond-** LYS B-210, SER B-209, ARG B-207, SER A-65, SER A-63, PHE B-250 **Salt-bridge-**LYS B-210 **Charged positive -**ARG A-64 **Charged negative-** ASN B-208, SER B-205, THR A-62, SER B-249

		Hydrophobic- PHE-256, TRP B-206, TRP B-214
	Epigallocatechin gallate	**H-Bond-** THR A-62, ARG B-207, ASN B-208, SER B-209, TRP B-214, GLU B-248 **Salt-bridge-** LYS B-210 **Charged positive-** ARG A-64 **Charged negative-** ASP B-211 **Polar-** HIE A-121, SER A-63, SER B-251, SER B-249 **Hydrophobic-** TRP B-206, PHE B-250, PHE B-256, PHE B-247 **Pi-cation-** ARG B-207 **Pi-pi stacking-** TRP B-206
	Rutin	**H-Bond-**SER A-63, LYS B-210, ARG B-207, SER B-205, PHE B-252, PHE B-250 **Charged positive -**ARG A-64 **Charged negative-** ASP B-253 **Polar-** SER A-65, THR A-62, SER B-209, ASN B-208, SER B-251, HIE A-121 **Hydrophobic-** CYS A-163, TRP B-206, TYR B-204, LEU A-168, PHE B-256
	prunasin	**H-Bond-**GLU A-130, THR A-331, ARG A-134, ACE C-1713, THR A-220 **Charged positive-**ARG A-134, 221, 279, 332 **Charged negative-**ASP A-131, 280 **Glycine –** GLY A-227 **Hydrophobic-**LEU A-132, LEU C-1715, VAL A-217, 218, PRO A-133, 219, 272, 330, TYR A-277, ALA A-333, ALA C-1714
	β-sitosterol	**H-Bond-**GLU-310, MET-341 **Charged positive-**LYS-295 **Charged negative-**ASP-404, GLU-339 **Polar-**SER-345, THR-338 **Glycine-**GLY-274, 344 **Hydrophobic-**LEU-273, 393, TYR-340, VAL-281, 323, ALA-293, 403, ILE-336, MET-314, PHE-405

3.4 Two-Dimensional Interaction Analysis

Two-dimensional (2D) interaction diagrams produced from the docked complexes were used to further visualize the molecular interactions between PARP1 and the chosen phytochemicals (Table 4). In addition to identifying the amino acid residues involved in hydrogen bonding, hydrophobic interactions, π–π stacking, π-cation interactions, and

water-mediated contacts, the diagrams clearly show how each ligand is oriented within the active-site cavity. The top-ranked compounds occupied the catalytic binding pocket in orientations that were advantageous for stable ligand binding, according to the 2D interaction diagrams. Vicenin-2 created a vast hydrogen-bonding network because of its glycosylated flavonoid structure, while isoquercetin and quercetin generated numerous hydrogen bonds through their hydroxyl groups. In contrast, amygdalin and prunasin generally interacted through hydrogen bonding involving their sugar moieties, whereas β-sitosterol primarily displayed hydrophobic interactions due to its stiff steroid nucleus. The docking scores and MM/GBSA binding free energy estimates accord with these interaction patterns, indicating that the discovered phytochemicals have advantageous structural characteristics for binding to PARP1's catalytic domain.

Table 4: Representing 2D-Interaction Diagrams

Protein	Compound	2D-Interaction Diagram
2RCW	Quercetin	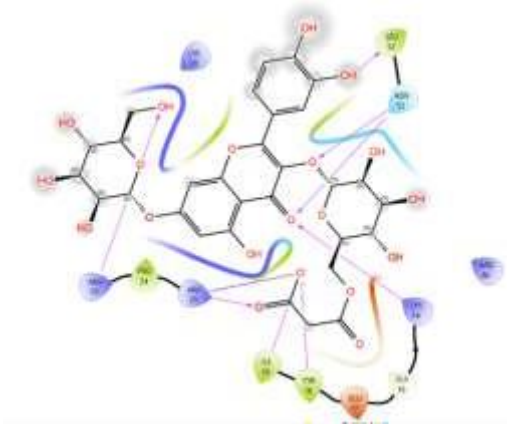
	Vicenin-2	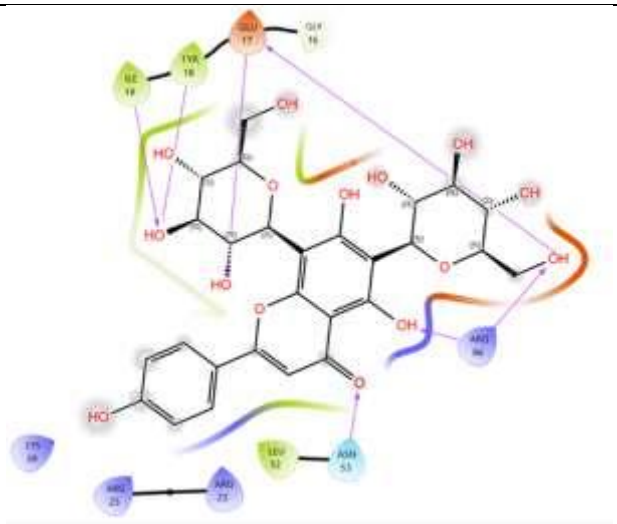

	Amygdalin	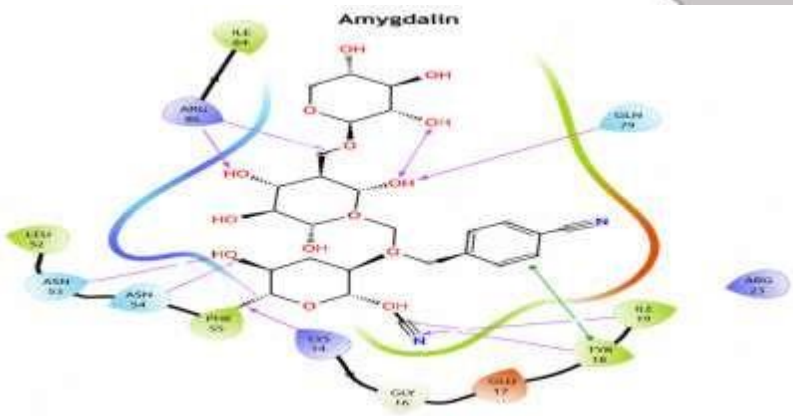
	isoquercetin	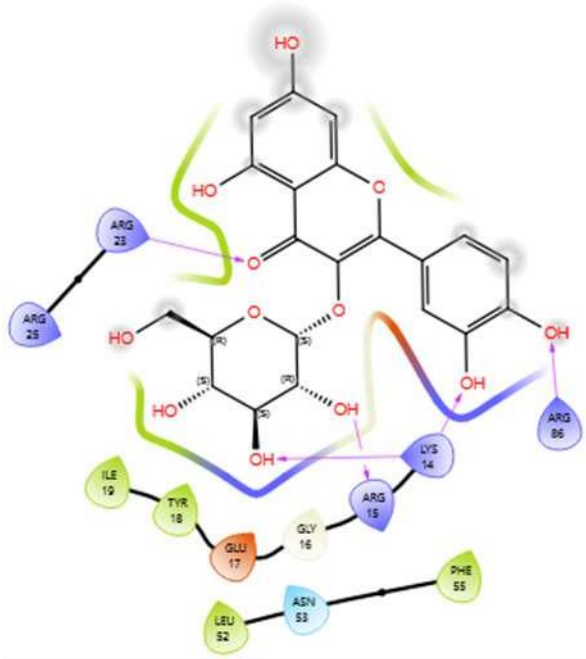

	kaempferol	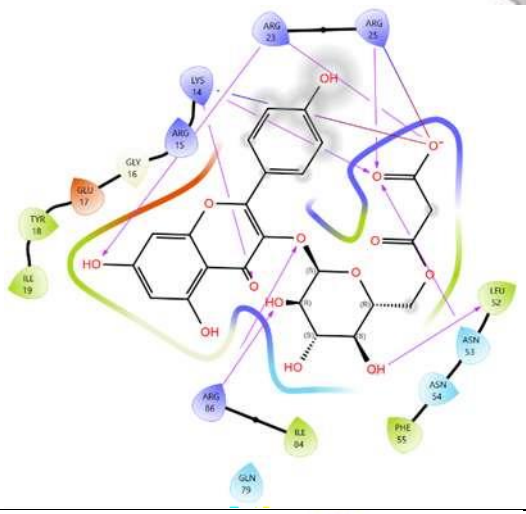
	Epigallocatechin gallate	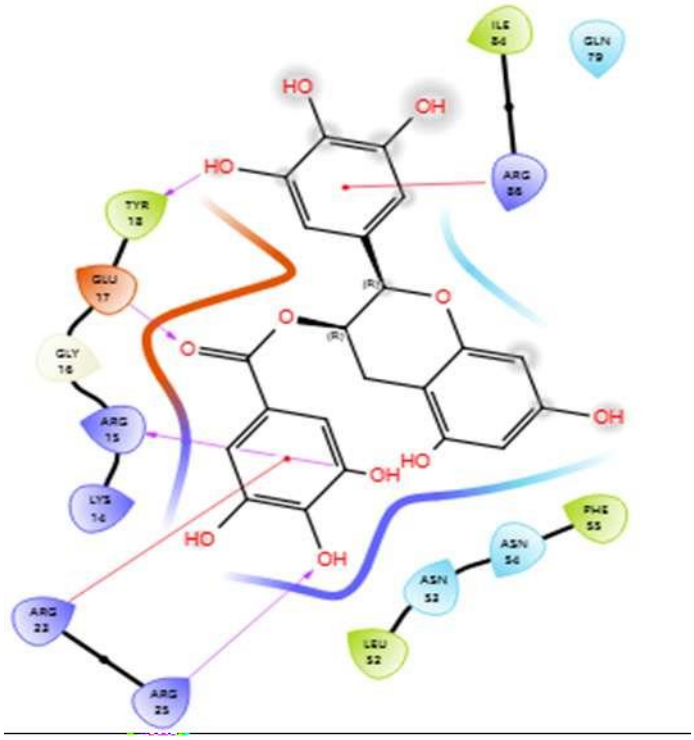

	Rutin	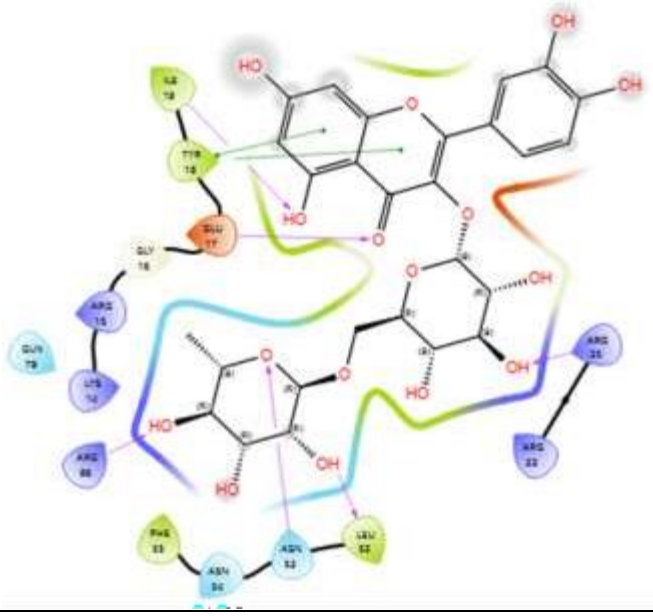
	prunasin	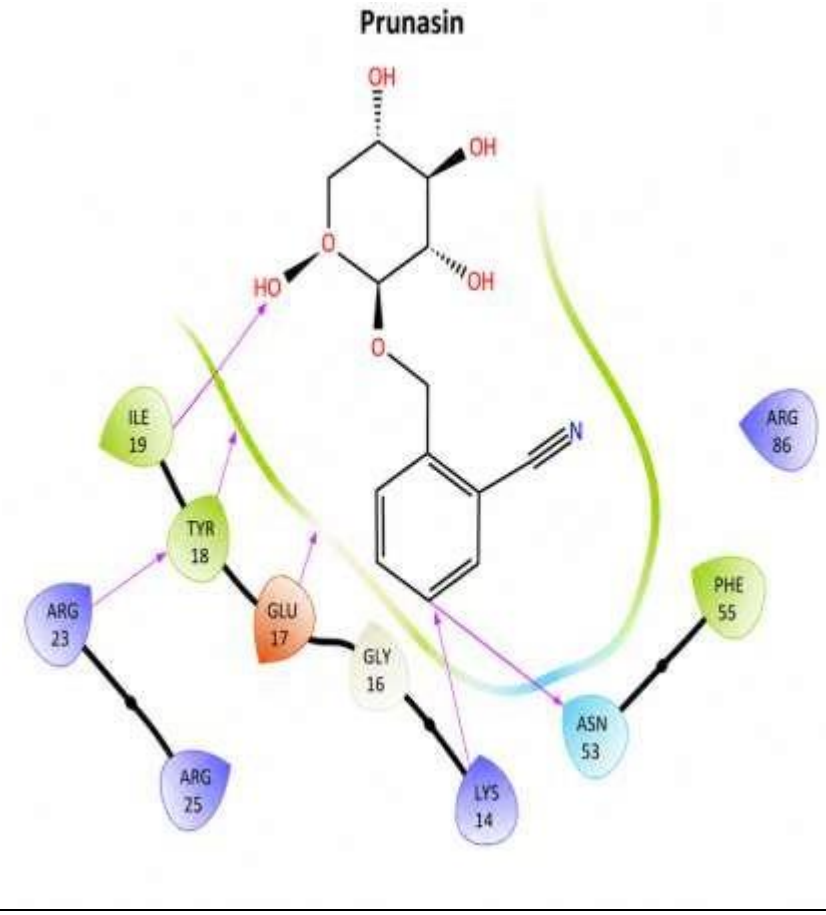

	β-sitosterol	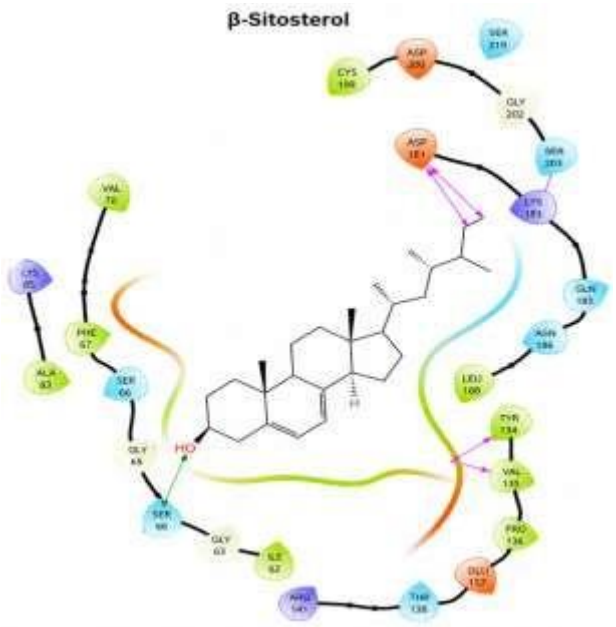

3.5 The Candidate Compounds PARP1 Enzymatic Activity

Inhibition of PARP1 by selected candidate compounds indicated concentration dependence. Among four candidate compounds, isoquercetin had the strongest ability to inhibit PARP1 with an IC50 value of 0.78± 0.12 0.8 µM (Fig. 1)

Figure 1:. Representing in-vitro inhibition of PARP1 by selected compounds

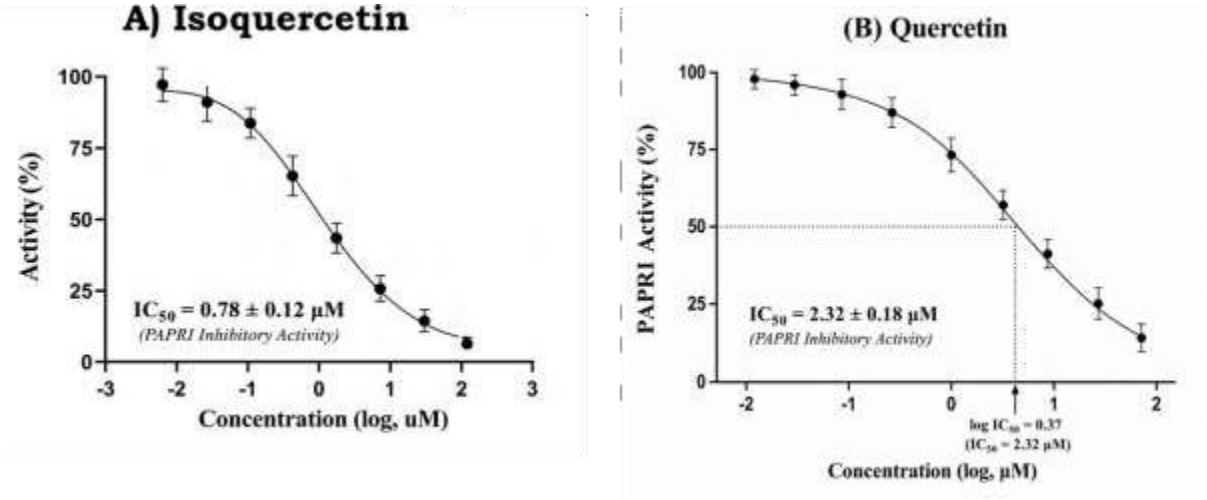

4.0 Conclusion

Structure-Based Virtual Screening of Bitter Almond Phytochemicals Against PARP1

PDVA consist active various phytochemicals among which on the basis of literature review we selected phytochemicals includes β-sitosterol, prunasin, rutin, epigallocatechin gallate, kaempferol, quercetin, isoquercetin, vicenin-2 and amygadin for molecular docking, binding free energy, ligand protein interactions and its 2D representation and selected in-vitro activity targeting PARP1 which results in under oxidative stress, reactive oxygen species (ROS) damage DNA, heavily over-activating PARP1. PARP1 then depletes cellular NAD^+ and ATP, triggering cell death. PARP1 inhibitors block this suicidal energy depletion, while simultaneously reducing inflammation.

Overall the best compound shows both molecular docking and in-vitro study against PARP1 is iso-quercetin.

5.0 References

1) Ray, C.A.; Nussenzweig, A. The multifaceted roles of PARP1 in DNA repair and chromatin remodelling. Nat. Rev. Mol. Cell Biol., 2017, 18(10), 610-621.
2) Alemasova, E.E.; Lavrik, O.I. Poly(ADP-ribosyl)ation by PARP1: Reaction mechanism and regulatory proteins. Nucleic Acids Res., 2019, 47(8), 3811-3827
3) Spiegel, J.O.; Van Houten, B.; Durrant, J.D. PARP1: Structural insights and pharmacological targets for inhibition. DNA Repair (Amst.), 2021, 103, 103125.
4) Dhahri, H.; Fondufe-Mittendorf, Y.N. Exploring the interplay between PARP1 and circRNA biogenesis and function. Wiley Interdiscip. Rev. RNA, 2024, 15(1), e1823.
5) Deeksha, W.; Rajakumara, E. Regulatory apoptotic fragment of PARP1 complements catalytic fragment for PAR and DNAdependent activity but inhibits DNA-induced catalytic stimulation of PARP2. DNA Repair (Amst.), 2024, 133, 103593.
6) Krug, S.; Gupta, M.; Kumar, P.; Feller, L.; Ihms, E.A.; Kang, B.G.Srikrishna, G.; Dawson, T.M.; Dawson, V.L.; Bishai, W.R. Inhibition of host PARP1 contributes to the anti- inflammatory and antitubercular activity of pyrazinamide. Nat. Commun., 2023, 14(1),208161.
7) Langelier, M.F.; Planck, J.L.; Roy, S.; Pascal, J.M. Structural basis for DNA damage-dependent poly(ADP-ribosyl)ation by human PARP-1. Science, 2012, 336(6082), 728-732.
8) Menear, K.A.; Adcock, C.; Boulter, R.; Cockcroft, X.; Copsey, L.; Cranston, A.; Dillon, K.J.; Drzewiecki, J.; Garman, S.; Gomez, S.; Javaid, H.; Kerrigan, F.; Knights, C.; Lau, A.; Loh, V.M.; Matthews, I.T.W.; Moore, S.; O'Connor, M.J.; Smith, G.C.M.; Martin, N.M.B. 4-[3-(4-cyclopropanecarbonylpiperazine-1-carbonyl)-4- fluorobenzyl]-2H-phthalazin-1-one: A novel bioavailable inhibitor of poly(ADP-ribose) polymerase-1. J. Med. Chem., 2008, 51(20), 6581-6591.
9) Thomas, H.D.; Calabrese, C.R.; Batey, M.A.; Canan, S.; Hostomsky, Z.; Kyle, S.; Maegley, K.A.; Newell, D.R.; Skalitzky, D.; Wang, L.Z.; Webber, S.E.; Curtin, N.J. Preclinical selection of a novel poly(ADP-ribose) polymerase inhibitor for clinical trial. Mol.Cancer Ther., 2007, 6(3), 945-956.
10) Jones, P.; Altamura, S.; Boueres, J.; Ferrigno, F.; Fonsi, M.; Giomini, C.; Lamartina, S.; Monteagudo, E.; Ontoria, J.M.; Orsale, M.V.; Palumbi, M.C.; Pesci, S.; Roscilli, G.; Scarpelli, R.; SchultzFademrecht, C.; Toniatti, C.; Rowley, M. Discovery of 2-{4-[(3S)-piperidin-3-yl]phenyl}-2H-indazole-7-carboxamide (MK-4827): A novel oral poly(ADP-ribose)polymerase (PARP) inhibitor efficacious in BRCA-1 and -2 mutant tumors. J. Med. Chem., 2009, 52(22), 7170-7185.
11) Litton, J.K.; Rugo, H.S.; Ettl, J.; Hurvitz, S.A.; Gonçalves, A.; Lee, K.H.; Fehrenbacher, L.; Yerushalmi, R.; Mina, L.A.; Martin, M.; Roché, H.; Im, Y.H.; Quek, R.G.W.; Markova, D.; Tudor, I.C.; Hannah, A.L.; Eiermann, W.; Blum, J.L. Talazoparib in patients with advanced breast cancer and a germline BRCA mutation. N.Engl. J. Med., 2018, 379(8), 753-763.
12) Agarwal, N.; Azad, A.A.; Carles, J.; Fay, A.P.; Matsubara, N.;Heinrich, D.; Szczylik, C.; De Giorgi, U.; Young Joung, J.; Fong, P.C.C.; Voog, E.; Jones, R.J.; Shore, N.D.; Dunshee, C.; Zschäbitz, S.; Oldenburg, J.; Lin, X.; Healy, C.G.; Di Santo, N.; Zohren, F.;Fizazi, K. Talazoparib plus enzalutamide in men with first-line metastatic castration-resistant prostate cancer (TALAPRO-2): A randomised, placebo-controlled, phase 3 trial. Lancet, 2023, 402(10398), 291-303.
13) Yuan, B.; Ye, N.; Song, S.S.; Wang, Y.T.; Song, Z.; Chen, H.D.; Chen, C.H.; Huan, X.J.; Wang, Y.Q.; Su, Y.; Shen, Y.Y.; Sun, Y.M.; Yang, X.Y.; Chen, Y.; Guo, S.Y.; Gan, Y.; Gao, Z.W.; Chen, X.Y.; Ding, J.; He, J.X.; Zhang, A.; Miao, Z.H Poly(ADPribose)polymerase (PARP) inhibition and anticancer activity of simmiparib, a new inhibitor undergoing clinical trials. Cancer Lett., 2017, 386, 47-56.
14) Donawho, C.K.; Luo, Y.; Luo, Y.; Penning, T.D.; Bauch, J.L.; Bouska, J.J.; Bontcheva-Diaz, V.D.; Cox, B.F.; DeWeese, T.L.; Dillehay, L.E.; Ferguson, D.C.; Ghoreishi-Haack, N.S.; Grimm, D.R.; Guan, R.; Han, E.K.; Holley-Shanks, R.R.; Hristov, B.; Idler, K.B.; Jarvis, K.; Johnson, E.F.; Kleinberg, L.R.; Klinghofer, V.; Lasko, L.M.; Liu, X.; Marsh, K.C.; McGonigal, T.P.; Meulbroek,J.A.; Olson, A.M.; Palma, J.P.; Rodriguez, L.E.; Shi, Y.; Stavropoulos, J.A.; Tsurutani,

A.C.; Zhu, G.D.; Rosenberg, S.H.; Giranda, V.L.; Frost, D.J. ABT-888, an orally active poly(ADPribose) polymerase inhibitor that potentiates DNA-damaging agents in preclinical tumor models. Clin. Cancer Res., 2007, 13(9), 2728- 2737.

15) Li, X.; Wang, C.; Li, S.; Yin, F.; Luo, H.; Zhang, Y.; Luo, Z.; Chen, Y.; Wan, S.; Kong, L.; Wang, X. Dual target PARP1/EZH2 inhibitors inducing excessive autophagy and producing synthetic lethality for triple-negative breast cancer therapy. Eur. J. Med.Chem., 2024, 265, 116054.
16) Zhang, L.; Zhen, Y.; Feng, L.; Li, Z.; Lu, Y.; Wang, G.; Ouyang, L. Discovery of a novel dual-target inhibitor of CDK12 and PARP1 that induces synthetic lethality for treatment of triple-negative breast cancer. Eur. J. Med. Chem., 2023, 259, 115648.
17) Zhang, J.; Zhang, J.; Li, H.; Chen, L.; Yao, D. Dual-target inhibitors of PARP1 in cancer therapy: A drug discovery perspective.Drug Discov. Today, 2023, 28(7), 103607.
18) Wang, P.; Zhu, W.T.; Wang, Y.; Song, S.S.; Xi, Y.; Yang, X.Y.; Shen, Y.Y.; Su, Y.; Sun, Y.M.; Gao, Y.L.; Chen, Y.; Ding, J.; Miao, Z.H.; Zhang, A.; He, J.X. Identification of [1,2,4]Triazolo[4,3- a]pyrazine PARP1 inhibitors with overcome acquired resistance activities. Eur. J. Med. Chem., 2023, 259, 115709.
19) Kim, C.; Wang, X.D.; Jang, S.; Yu, Y. PARP1 inhibitors induce pyroptosis via caspase 3-mediated gasdermin E cleavage. Biochem. Biophys. Res. Commun., 2023, 646, 78-85.
20) Kellett, T.; Noor, R.; Zhou, Q.; Esquer, H.; Sala, R.; Stojanovic, P.; Rudolph, J.; Luger, K.; LaBarbera, D.V. HTS discovery of PARP1-HPF1 complex inhibitors in cancer. SLAS Discov., 2023, 28(8),394-401.
21) Peng, X.; Pan, W.; Jiang, F.; Chen, W.; Qi, Z.; Peng, W.; Chen, J.Selective PARP1 inhibitors, PARP1-based dual-target inhibitors, PROTAC PARP1 degraders, and prodrugs of PARP1 inhibitors for cancer therapy. Pharmacol. Res., 2022, 186, 106529.
22) Liu, X.; Wei, X.; Li, X.; Yu, R.; Jiang, T.; Zhao, C. Design, synthesis, and bioactivity study on Lissodendrins B derivatives as PARP1 inhibitor. Bioorg. Med. Chem., 2022, 69, 116892.
23) Li, G.; Lin, S.; Yu, Z.; Wu, X.; Liu, J.; Tu, G.; Liu, Q.; Tang, Y.; Jiang, Q.; Xu, J.; Huang, Q.; Wu, L. A PARP1 PROTAC as a novel strategy against PARP inhibitor resistance via promotion of ferroptosis in p53-positive breast cancer. Biochem. Pharmacol., 2022, 206, 115329.
24) Kayumov, M.; Jia, L.; Pardaev, A.; Song, S.S.; Mirzaakhmedov, S.; Ding, C.; Cheng, Y.J.; Zhang, R.I.; Bao, X.; Miao, Z.H.; He, J.X.; Zhang, A. Design, synthesis and pharmacological evaluation of new PARP1 inhibitors by merging pharmacophores of olaparib and the natural product alantolactone. Eur. J. Med. Chem., 2022, 240, 114574.
25) Eldin A Osman, E.; Hanafy, N.S.; George, R.F.; El-Moghazy, S.M.; El-Moghazy, S.M. Design and synthesis of some barbituric and 1,3-dimethylbarbituric acid derivatives: A non-classical scaffold for potential PARP1 inhibitors. Bioorg. Chem., 2020, 104, 104198.
26) Jain, P.G.; Patel, B.D. Medicinal chemistry approaches of poly ADP-Ribose polymerase 1 (PARP1) inhibitors as anticancer agents - A recent update. Eur. J. Med. Chem., 2019, 165, 198-215.
27) Langelier, M.F.; Zandarashvili, L.; Aguiar, P.M.; Black, B.E.; Pascal, J.M. NAD+ analog reveals PARP-1 substrate-blocking mechanism and allosteric communication from catalytic center to DNA-binding domains. Nat. Commun., 2018, 9(1), 844.
28) Asiamah, I.; Obiri, S.A.; Tamekloe, W.; Armah, F.A.; Borquaye,L.S. Applications of molecular docking in natural products-based drug discovery. Sci. Am., 2023, 20, e01593.
29) Kaur, T.; Madgulkar, A.; Bhalekar, M.; Asgaonkar, K. Molecular docking in formulation and development. Curr. Drug Discov.Technol., 2019, 16(1), 30-39.
30) Saikia, S.; Bordoloi, M. Molecular docking: Challenges, advances and its use in drug discovery perspective. Curr. Drug Targets,2019, 20(5), 501-521.
31) Putt, K. S., & Hergenrother, P. J. (2004). An enzymatic assay for poly(ADP-ribose) polymerase-1 (PARP-1) via the chemiluminescent detection of NAD^+ consumption. Analytical Biochemistry, 326(1), 78–86. https://doi.org/10.1016/j.ab.2003.11.019